

Two-Dimensional Analytical Model for Deriving the Threshold Voltage of a Short Channel Fully Depleted Cylindrical/Surrounding Gate MOSFET

Chung Ha Suh

Abstract—A two-dimensional analytical model for deriving the threshold voltage of a short channel fully depleted (FD) cylindrical/surrounding gate MOSFET (CGT/SGT) is suggested. By taking into account the lateral variation of the surface potential, introducing the natural length expression, and using the Bessel functions of the first and the second kinds of order zero, we can derive potentials in the gate oxide layer and the silicon core fully two-dimensionally. Making use of these potentials, the minimum surface potential can be obtained to derive the threshold voltage as a closed-form expression in terms of various device parameters and applied voltages. Obtained results can be used to explain the drain-induced threshold voltage roll-off of a CGT/SGT in a unified manner.

Index Terms—Short channel cylindrical/surrounding gate MOSFET, CGT/SGT, natural length, drain-induced threshold voltage roll-off

I. INTRODUCTION

Recently, a surrounding gate MOSFET (SGT) has drawn much attention because of its fundamental advantages. Compared with conventional planar MOSFETs, SGTs have several superior characteristics such as high packing density, high current drive capability, and immunity to the short channel effect [1-6]. In a cylindrical/surrounding gate MOSFET (CGT/SGT),

a rectangular-shaped silicon core in the original SGT has been replaced with a cylindrical silicon core (pillar). Then due to the cylindrical structure, a CGT/SGT can avoid the narrow gate effect. This unique feature may give potentiality to play an important role in ULSI. Moreover, cylindrical/surrounding gate MOSFETs have been popularly considered nowadays since they can be yarn-type (flexible) electronic devices and can provide noticeable possibility for the application to textile (woven) electronics. However, as the channel length is shortened into the deep sub-micrometer regime, the short channel effects become significant. Among the several short channel effects, the drain-induced threshold voltage roll-off is the most important and principally due to the lateral field effect. An accurate estimation of the threshold voltage for a FET is crucial in the device optimization for circuit design. In most of analytical models [7-14], the threshold voltage of a short channel fully depleted (FD) cylindrical/surrounding gate MOSFET has been derived based upon the drain-induced barrier lowering (DIBL). The two-dimensional (2-D) Poisson's equation in the silicon core has been solved by decomposing it into a 1-D Poisson's equation and a 2-D Laplace's equation. In solving the 2-D Laplace's equation, however, complicated Fourier-Bessel series expansion has been required in order to satisfy the suggested equi-potential boundary conditions at both planes of source-core and drain-core $n^+ - p$ junctions. Hence, the surface potential has been expressed as a certain infinite series expansion, which has been approximated by taking only one term in the derivation of the minimum surface potential. This approximation

seems to be oversimplified and may be inconsistent with the suggested equi-potential boundary conditions. On the other hand, in several models [9, 13], it has been assumed that the potential in the silicon core can be expressed as a parabolic function of the radial coordinate. This parabolic expression assumption, even though can avoid the complexity involved in [12, 14], will be somewhat oversimplified since the potential in the silicon core has been derived by satisfying the 2-D Poisson's equation only at the silicon/oxide interface. Moreover, in most of previously suggested analytical models, the potential in the oxide layer has been derived by using the GCA (gradual channel approximation). However, the GCA-used solution may not be an appropriate solution of the 2-D Laplace equation since the GCA may not be applicable to the 2-D Laplace equation in a short and thick oxide layer.

In this paper, starting from the GCA-used potential expressions in the gate oxide layer and the silicon core, updating them iteratively by taking into account the lateral variation of the surface potential, introducing the natural length expression, and using the Bessel functions of the first and the second kinds of order zero, we can derive potentials in the oxide layer and the silicon core fully two-dimensionally. Making use of these potentials, the minimum surface potential can be obtained to derive the threshold voltage as a closed-form in terms of various device parameters and applied voltages. The simulation results of the presented model show fairly good agreement with the simulation results given in [14] except some noticeable discrepancies in the range of shorter channel length with lighter doping density in the silicon core, thicker silicon core, and thicker oxide layer.

This paper is organized as follows. In Section II, the basic model formulation is described. In Section III, typical computation results are shown. Section IV contains a summary of the conclusions.

II. MODEL FORMULATION

A schematic cross section of a cylindrical/surrounding gate MOSFET is shown in Fig. 1. Here r is the radial coordinate from the center axis of the cylindrical core toward the gate layer; y is the longitudinal coordinate from the source toward the drain; L is the channel length; $r_s = t_{si} / 2$ is the silicon core radius; t_{ox} is the

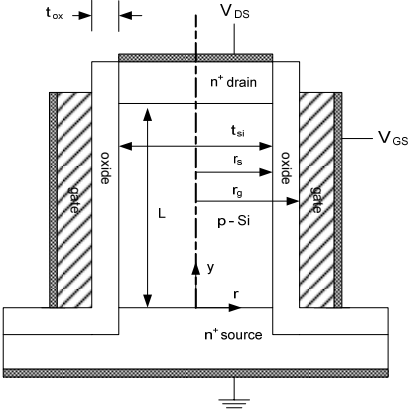


Fig. 1. Schematic cross-section view of an n-channel cylindrical/surrounding gate MOSFET to be modeled.

gate oxide layer thickness; $r_g = r_s + t_{ox}$; V_{GS} and V_{DS} are gate and drain voltages, respectively. In order to establish an accurate and rigorous threshold voltage model for a short channel fully depleted (FD) cylindrical/surrounding gate MOSFET, let us assume that the space charge density in the gate oxide layer is negligible and the silicon core is uniformly p-doped and fairly thin so that the silicon core is fully depleted in the sub-threshold regime. Then we can use the following 2-D Laplace/Poisson's equation:

$$\frac{1}{r} \frac{\partial}{\partial r} \left(r \frac{\partial \psi}{\partial r} \right) + \frac{\partial^2 \psi}{\partial y^2} = \begin{cases} 0, & r_s \leq r \leq r_g, \\ \frac{qN_A}{\epsilon_{si}}, & 0 \leq r \leq r_s, \end{cases} \quad (1)$$

where $\psi(r, y)$ is the 2-D (actually, 3-dimensional because of the symmetry about the polar angle) electrostatic potential, q is the elementary charge, N_A is the uniform acceptor density in the p-silicon core, and ϵ_{si} is the silicon dielectric constant. Boundary conditions subject to Eq. (1) are as follows:

$$\psi^{ox}(r_g, y) = V_{GS} - \varphi_{ms} = V_{GS}', \quad (2)$$

$$\psi^{si}(r_s, y) = \psi^{ox}(r_s, y) = \psi_s(y), \quad (3)$$

$$\left. \frac{\partial \psi^{si}}{\partial r} \right|_{r=0} = 0, \quad (4)$$

$$\mathcal{E}_{si}(y) = \eta \mathcal{E}_{ox}(y) - \frac{Q_{ss}}{\epsilon_{si}}, \quad (5)$$

where $\psi^{ox}(r, y)$ is the potential in the oxide layer, $\psi^{si}(r, y)$ is the potential in the silicon core, $\varphi_m - \varphi_s$ is the difference between the work functions (written in volts) φ_m for the gate and φ_s for the silicon core, $\psi_s(y)$ is the surface potential, $\mathcal{E}_{si}(y) = -\partial\psi^{si}/\partial r|_{r=r_s}$, $\mathcal{E}_{ox}(y) = -\partial\psi^{ox}/\partial r|_{r=r_s}$, $\eta = \epsilon_{ox}/\epsilon_{si}$, ϵ_{ox} is the dielectric constant of oxide, and Q_{ss} is the surface state charge density at the silicon/oxide interface. In order to derive both $\psi^{si}(r, y)$ and $\psi^{ox}(r, y)$ fully two-dimensionally, let us start from the GCA-used potential expressions $\psi^{si}(r, y)$ and $\psi^{ox}(r, y)$ of the forms:

$$\psi^{si}(r, y) \approx \frac{qN_A}{4\epsilon_{si}}(r^2 - r_s^2) + f_0(r)\psi_s(y), \quad (6)$$

$$\psi^{ox}(r, y) \approx V_{GS}' [1 - g_0(r)] + g_0(r)\psi_s(y), \quad (7)$$

where

$$f_0(r) = 1, \quad (8)$$

$$g_0(r) = \frac{\ln(r_g/r)}{\ln(r_g/r_s)}. \quad (9)$$

Differentiating Eqs. (6, 7) twice with respect y yields

$$\frac{\partial^2 \psi^{si}}{\partial y^2} \approx f_0(r) \frac{d^2 \psi_s}{dy^2}, \quad (10)$$

$$\frac{\partial^2 \psi^{ox}}{\partial y^2} \approx g_0(r) \frac{d^2 \psi_s}{dy^2}. \quad (11)$$

Substituting Eqs. (10, 11) into the lower and upper parts of Eq. (1), respectively, and considering Eqs. (2-4), we can update Eqs. (6, 7) once. Performing the similar procedures iteratively, we can write $\psi^{si}(x, y)$ and $\psi^{ox}(x, y)$ in the following GCA-free expressions:

$$\psi^{si}(r, y) = \frac{qN_A}{4\epsilon_{si}}(r^2 - r_s^2) + \sum_{n=0}^{\infty} (-1)^n f_n(r) \frac{d^{2n} \psi_s}{dy^{2n}}, \quad (12)$$

$$\psi^{ox}(r, y) = V_{GS}' [1 - g_0(r)] + \sum_{n=0}^{\infty} (-1)^n g_n(r) \frac{d^{2n} \psi_s}{dy^{2n}}, \quad (13)$$

where $f_n(r)$ and $g_n(r)$ for $n=1, 2, 3, \dots$ are of the forms:

$$f_n(r) = \int_{r_s}^r \left[\frac{1}{r'} \int_0^{r'} r' f_{n-1}(r') dr' \right] dr', \quad (14)$$

$$g_n(r) = \int_{r_s}^r \left[\frac{1}{r'} \int_{r_s}^{r'} r' g_{n-1}(r') dr' \right] dr' - \frac{\ln(r/r_s)}{\ln(r_g/r_s)} \int_{r_s}^{r_g} \left[\frac{1}{r'} \int_{r_s}^{r'} r' g_{n-1}(r') dr' \right] dr', \quad (15)$$

which can be obtained by considering that

$$\left. \frac{df_n}{dr} \right|_{r=0} = 0, \quad (16a)$$

$$f_n(r_s) = 0, \quad (16b)$$

$$\frac{1}{r} \frac{d}{dr} \left(r \frac{df_n}{dr} \right) = f_{n-1}(r), \quad (16c)$$

$$g_n(r_s) = 0, \quad (17a)$$

$$g_n(r_g) = 0, \quad (17b)$$

$$\frac{1}{r} \frac{d}{dr} \left(r \frac{dg_n}{dr} \right) = g_{n-1}(r). \quad (17c)$$

Differentiating Eqs. (12, 13) with respect to r and putting $r = r_s$, we get

$$\mathcal{E}_{si}(y) = -\frac{qN_A r_s}{2\epsilon_{si}} - \sum_{n=1}^{\infty} (-1)^n f_{n,s} \frac{d^{2n} \psi_s}{dy^{2n}}, \quad (18)$$

$$\mathcal{E}_{ox}(y) = -\frac{1}{\sigma r_s} \left[V_{GS}' - \psi_s(y) \right] - \sum_{n=1}^{\infty} (-1)^n g_{n,s} \frac{d^{2n} \psi_s}{dy^{2n}}, \quad (19)$$

where

$$\sigma = \ln \left(\frac{r_g}{r_s} \right) = \ln \left(1 + \frac{t_{ox}}{r_s} \right), \quad (20)$$

$$f'_{n,s} = \frac{df_n}{dr} \Big|_{r=r_s} = \frac{1}{r_s} \int_0^{r_s} r f_{n-1}(r) dr, \quad (21)$$

$$g'_{n,s} = \frac{dg_n}{dr} \Big|_{r=r_s} = -\frac{1}{\sigma r_s} \int_{r_s}^{r_g} \left[\frac{1}{r'} \int_{r_s}^{r'} r g_{n-1}(r) dr \right] dr'. \quad (22)$$

Substituting Eqs. (18, 19) into Eq. (5), we can get the following linear differential equation:

$$\psi_s(y) - \Phi_s - \sum_{n=1}^{\infty} a_n \frac{d^{2n} \psi_s}{dy^{2n}} = 0, \quad (23)$$

where Φ_s and a_n are defined by

$$\Phi_s = V_{GS} - \varphi_{ms} + \frac{\sigma r_s Q_{ss}}{\epsilon_{ox}} - \frac{q N_A \sigma r_s^2}{2 \epsilon_{ox}}, \quad (24)$$

$$a_n = -(-1)^n \sigma r_s \left(\frac{1}{n} f'_{n,s} - g'_{n,s} \right). \quad (25)$$

In order to find the solution $\psi_s(y)$ of Eq. (23), we can suggest that

$$\frac{d^2 \psi_s}{dy^2} = \frac{1}{\lambda^2} [\psi_s(y) - \Phi_s], \quad (26)$$

where λ is referred to as the natural (or characteristic) length that can be determined by solving the following characteristic equation:

$$1 - \sum_{n=1}^{\infty} a_n \lambda^{-2n} = 0. \quad (27)$$

Neglecting all terms $a_n \lambda^{-2n}$ for $n \geq 4$ in Eq. (27), we can approximate Eq. (27) as the cubic equation of $\xi = \lambda^2$:

$$\xi^3 - a_1 \xi^2 - a_2 \xi - a_3 \approx 0, \quad (28)$$

where a_1 , a_2 , and a_3 are given in Appendix I. Since

$a_1 > 0$, $a_2 > 0$, $a_3 > 0$, and $a_2^2 - 3a_1 a_3 < 0$, we can obtain the unique positive λ approximately given by

$$\lambda \approx \sqrt{\frac{a_1}{3} + \sqrt[3]{R + \sqrt{Q^3 + R^2}} + \sqrt[3]{R - \sqrt{Q^3 + R^2}}}, \quad (29)$$

$$\text{where } Q = -(3a_2 + a_1^2)/9 \quad \text{and} \quad R = (9a_1 a_2 + 2a_1^3 + 27a_3)/54.$$

However, since $f_n(r)$ and $g_n(r)$ for $n \geq 1$ can be derived only step by step and the expressions for a_n 's are complicated, we need another approach for the derivation of λ . To do this, let us substitute Eq. (26) into Eqs. (12, 13), and consider Eqs. (8, 9, 14, 15). Then we can rewrite Eqs. (12, 13), respectively, in the following closed-forms:

$$\psi^{si}(r, y) = \frac{qN_A}{4\epsilon_{si}} (r^2 - r_s^2) + \Phi_s + S(r) [\psi_s(y) - \Phi_s], \quad (30)$$

$$\psi^{ox}(r, y) = \frac{1}{\sigma} (V_{GS} - \Phi_s) \ln \left(\frac{r}{r_s} \right) + \Phi_s + T(r) [\psi_s(y) - \Phi_s], \quad (31)$$

where $S(r)$ and $T(r)$ are defined by

$$S(r) = \sum_{n=0}^{\infty} (-1)^n f_n(r) \lambda^{-2n}, \quad (32)$$

$$T(r) = \sum_{n=0}^{\infty} (-1)^n g_n(r) \lambda^{-2n}, \quad (33)$$

which satisfy $S(r_s) = 1$, $dS/dr|_{r=0} = 0$, $T(r_s) = 1$, $T(r_g) = 0$, and

$$\frac{d^2 S}{dr^2} + \frac{1}{r} \frac{dS}{dr} + \frac{S(r)}{\lambda^2} = 0, \quad (34)$$

$$\frac{d^2 T}{dr^2} + \frac{1}{r} \frac{dT}{dr} + \frac{T(r)}{\lambda^2} = 0. \quad (35)$$

By setting $x = r/\lambda$, Eqs. (34, 35) become Bessel's differential equations of order zero. Thus, we can have

$$S(r) = AJ_0(x) + BY_0(x) = \frac{J_0(x)}{J_0(x_s)}, \quad (36)$$

$$T(r) = CJ_0(x) + DY_0(x) = \frac{Y_0(x_g)J_0(x) - J_0(x_g)Y_0(x)}{J_0(x_s)Y_0(x_g) - J_0(x_g)Y_0(x_s)}, \quad (37)$$

where $x_s = r_s / \lambda$, $x_g = r_g / \lambda$, and $J_0(x)$ and $Y_0(x)$ are the Bessel functions of the first and the second kinds of order zero, respectively. In Eq. (36), we have used $dJ_0/dx|_{x=0} = 0$ and $dY_0/dx|_{x=0} = \infty$. After substituting Eqs. (36, 37) into Eqs. (30, 31), respectively, differentiating Eqs. (30, 31) with respect to r and putting $r = r_s$, we can rewrite Eqs. (18, 19), respectively, in the following closed-forms:

$$\mathcal{E}_{si}(y) = -\frac{qN_A r_s}{2\epsilon_{si}} + \frac{1}{\lambda} \frac{J_1(x_s)}{J_0(x_s)} [\psi_s(y) - \Phi_s], \quad (38)$$

$$\begin{aligned} \mathcal{E}_{ox}(y) = & -\frac{V'_{GS} - \Phi_s}{\sigma r_s} \\ & + \frac{1}{\lambda} \frac{Y_0(x_g)J_1(x_s) - J_0(x_g)Y_1(x_s)}{J_0(x_s)Y_0(x_g) - J_0(x_g)Y_0(x_s)} [\psi_s(y) - \Phi_s], \end{aligned} \quad (39)$$

where $J_1(x_s)$ and $Y_1(x_s)$ are the values at $x = x_s$ for the Bessel functions of the first and the second kinds of order 1, respectively. Substituting Eqs. (38, 39) into Eq. (5) and using Eq. (24), we can obtain

$$\frac{J_1(x_s)}{\eta J_0(x_s)} = \frac{Y_0(x_g)J_1(x_s) - J_0(x_g)Y_1(x_s)}{J_0(x_s)Y_0(x_g) - J_0(x_g)Y_0(x_s)}. \quad (40)$$

From Eq. (40), we can derive λ exactly. However, since all of $Y_0(x_g)J_1(x_s)$, $J_0(x_g)Y_1(x_s)$, $J_0(x_s)Y_0(x_g)$, and $J_0(x_g)Y_0(x_s)$ are very complicated functions of λ , Eq. (40) seems to be cumbersome in deriving λ . In order to derive λ more easily, let us use the following Taylor's series expansions:

$$J_0(x_g) = J_0(x_s + \tau x_s) = \sum_{k=0}^{\infty} \frac{1}{k!} (\tau x_s)^k J_0^{(k)}(x_s), \quad (41)$$

$$Y_0(x_g) = Y_0(x_s + \tau x_s) = \sum_{k=0}^{\infty} \frac{1}{k!} (\tau x_s)^k Y_0^{(k)}(x_s), \quad (42)$$

where $\tau = (x_g - x_s)/x_s$, $J_0^{(k)}(x_s) = d^k J_0/dx^k|_{x=x_s}$, and

$Y_0^{(k)}(x_s) = d^k Y_0/dx^k|_{x=x_s}$. Then using $dJ_0/dx = -J_1(x)$, $dJ_1/dx = J_0(x) - J_1(x)/x$, $dY_0/dx = -Y_1(x)$, and $dY_1/dx = Y_0(x) - Y_1(x)/x$ [15], we can have (see Appendix II)

$$J_0^{(k)}(x) = \mu_k(x)J_0(x) + \nu_k(x)J_1(x), \quad (43)$$

$$Y_0^{(k)}(x) = \mu_k(x)Y_0(x) + \nu_k(x)Y_1(x), \quad (44)$$

where $\mu_0(x) = 1$, $\nu_0(x) = 0$, and

$$\mu_k(x) = \frac{d\mu_{k-1}}{dx} + \nu_{k-1}(x), \quad k = 1, 2, 3, \dots, \quad (45)$$

$$\nu_k(x) = -\mu_{k-1}(x) + \frac{d\nu_{k-1}}{dx} - \frac{\nu_{k-1}(x)}{x}, \quad k = 1, 2, 3, \dots \quad (46)$$

Then Eq. (40) can be rewritten as

$$\sum_{k=0}^{\infty} \frac{1}{k!} \tau^k x_s^k [\eta \mu_k(x_s)J_0(x_s) + \nu_k(x_s)J_1(x_s)] = 0. \quad (47)$$

Since $\Delta x = \tau x_s \ll x_s$ is usually valid, the above infinite summation may be replaced with the truncated summation of $\sum_{k=0}^3 (\tau^k x_s^k / k!) [\eta \mu_k(x_s)J_0(x_s) + \nu_k(x_s)J_1(x_s)]$, within a range of satisfactory accuracy. Then using $\mu_0(x_s) = 1$, $\nu_0(x_s) = 0$, $\mu_1(x_s) = 0$, $\nu_1(x_s) = -1$, $\mu_2(x_s) = -1$, $\nu_2(x_s) = 1/x_s$, $\mu_3(x_s) = 1/x_s$, and $\nu_3(x_s) = 1 - 2/x_s^2$, Eq. (47) can be approximated as

$$\begin{aligned} & \eta \left(1 - \frac{1}{2} \tau^2 x_s^2 + \frac{1}{6} \tau^3 x_s^3 \right) J_0(x_s) \\ & + \left(-\tau x_s + \frac{1}{2} \tau^2 x_s^2 - \frac{1}{3} \tau^3 x_s^3 + \frac{1}{6} \tau^4 x_s^4 \right) J_1(x_s) \approx 0. \end{aligned} \quad (48)$$

Solving Eq. (48) by means of the Newton-Raphson method and choosing the smallest value of x_s (λ as the largest value), we can determine λ uniquely. It is worth pointing out that Eq. (48) can be solved much more easily than Eq. (40).

On the other hand, solving Eq. (26) gives

$$\psi_s(y) = \Phi_s + \frac{(\psi_{s0} - \Phi_s) \sinh\left(\frac{L-y}{\lambda}\right) + (\psi_{sL} - \Phi_s) \sinh\left(\frac{y}{\lambda}\right)}{\sinh\left(\frac{L}{\lambda}\right)}, \quad (49)$$

where $\psi_{s0} = \psi_s(0)$ and $\psi_{sL} = \psi_s(L)$. Performing some algebraic procedure [16, 17] upon Eq. (49), the minimum surface potential $\psi_{s,\min} = \psi_s(y_m)$ and the channel position $y = y_m$ can be derived as

$$\psi_{s,\min} = \Phi_s + (\psi_{s0} - \Phi_s) \sqrt{1 - \left[\tanh\left(\frac{L}{2\lambda}\right) - \frac{\psi_{sL} - \psi_{s0}}{\psi_{s0} - \Phi_s} \operatorname{csch}\left(\frac{L}{\lambda}\right) \right]^2}, \quad (50)$$

$$y_m = \frac{L}{2} - \lambda \tanh^{-1} \left[\frac{\psi_{sL} - \psi_{s0}}{\psi_{s0} + \psi_{sL} - 2\Phi_s} \coth\left(\frac{L}{2\lambda}\right) \right]. \quad (51)$$

Since ohmic drops due to the parasitic source and drain resistances can be neglected in the sub-threshold regime, $\psi_{s0} = V_{bi}$ and $\psi_{sL} = V_{bi} + V_{DS}$ can be used, where V_{bi} is the built-in voltage across the $n^+ - p$ source (drain)/channel junction. In case that both source and drain regions are uniformly doped with the same donor doping level N_D , we can have $V_{bi} = (k_B T / q) \ln(N_A N_D / n_i^2)$, where k_B is Boltzmann's constant, T is the absolute temperature, and n_i is the intrinsic carrier density of silicon. Consider that Eq. (50) for a long channel device ($L \gg \lambda$) becomes $\psi_{s,\min} \approx \Phi_s$ and that the threshold voltage for a long channel CGT/SGT, V_{T_∞} , is readily given by

$$V_{T_\infty} = \varphi_{ms} - \frac{Q_{ss}}{C_{ox}^{cyl}} + \frac{qN_A t_{si}}{4C_{ox}^{cyl}} + 2\Phi_B, \quad (52)$$

where $C_{ox}^{cyl} = \epsilon_{ox}/(\sigma r_s)$ and $\Phi_B = (k_B T / q) \ln(N_A / n_i)$. Then we can suggest that the sub-threshold condition, i.e., $V_{GS} \leq V_T$ will be equivalent to $\psi_{s,\min} \leq 2\Phi_B$. Thus, plugging Eq. (50) into $\psi_{s,\min} \leq 2\Phi_B$ and using Eq. (24), the threshold voltage, V_T , can be finally derived as

$$V_T = V_{T_\infty} - \left(\frac{1}{2} \psi_{s0} + \frac{1}{2} \psi_{sL} - 2\Phi_B \right) \operatorname{csch}^2\left(\frac{L}{2\lambda}\right) - \sqrt{(\psi_{s0} - 2\Phi_B)(\psi_{sL} - 2\Phi_B)} \coth\left(\frac{L}{2\lambda}\right) \operatorname{csch}\left(\frac{L}{2\lambda}\right). \quad (53)$$

III. SAMPLE COMPUTATION AND DISCUSSION

According to the expressions derived in Sec. II, the natural length λ and the threshold voltage V_T are computed and plotted in Figs. 2-7. In these computations, the following constants are used: $k_B T / q = 0.0259 V$, $n_i = 1.45 \times 10^{10} \text{ cm}^{-3}$, $\epsilon_{si} = 11.8 \times 8.85 \times 10^{-14} \text{ F/cm}$, and $\epsilon_{ox} = 3.9 \times 8.85 \times 10^{-14} \text{ F/cm}$. In order to compare the obtained simulation results with the simulated results in [14], the values of device parameters have been chosen to be the same values used in the model under comparison. For the values not given clearly, we have used $N_D = 1 \times 10^{19} \text{ cm}^{-3}$, $Q_{ss} = 6.4 \times 10^{-9} \text{ C/cm}^2$, and $\varphi_{ms} = -(0.55 + \Phi_B)V$ (n^+ -poly silicon gate). In Fig. 2, the values λ derived according to Eqs. (29, 48), respectively, are plotted as functions of t_{ox}/t_{si} ($t_{si} = 40 \text{ nm}$) and compared with the result given in [11]. The values a_1 , a_2 , and a_3 used in Eq. (29) are given by Eqs. (I-10, I-11, I-12) derived in Appendix I. In this figure, it can be shown that Eq. (48) gives excellent agreement with the PADRE simulation result given in [11] while Eq. (29) seems to be less accurate than Eq. (48) in the range of thinner oxide layer. The surface potential $\psi_s(y)$ for a long channel ($L = 0.5 \mu\text{m}$) and a short channel ($L = 0.1 \mu\text{m}$) devices are plotted in Fig. 3. The dependence of the threshold voltage on the channel length for various values of drain voltage is plotted in Fig. 4. In Fig. 3 and Fig. 4, the computation results of the presented model are compared with the results calculated by using Eqs. (9, 13) given in [14]. In these figures, noticeable discrepancies are shown in the range of shorter channel length. The derived dependences of the threshold voltage roll-off, $V_{T_\infty} - V_T$, on the channel length for various values of doping density in the silicon core, silicon core diameter, and oxide layer thickness are shown in Fig. 5, Fig. 6 and Fig. 7, respectively. The simulation results of the present model show noticeable disagreement with the results given in [14], especially in the range of shorter channel length with lighter doping density in the silicon core, thicker silicon core, and

thicker oxide layer. These discrepancies may result from the fact that the presented model derives the surface potential as a simple closed-form expression that does not need any approximation while the model under comparison derived the surface potential as an approximated form containing noticeable mismatches at both surface channel ends by oversimplifying the infinite series expansion form.

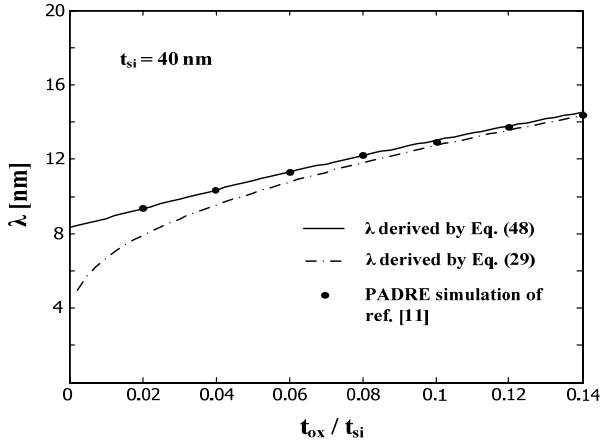


Fig. 2. Derived λ according to Eqs. (29) and (48) are plotted as functions of t_{ox}/t_{si} ($t_{si} = 40\text{ nm}$) and compared with the result given in [11]. The values a_1 , a_2 , and a_3 in Eq. (29) are used according to Eqs. (I-10), (I-11), and (I-12) derived in Appendix I.

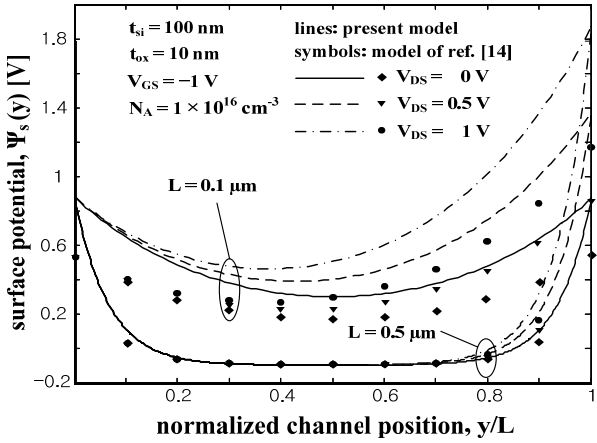


Fig. 3. Surface potential profiles for a typical long channel ($L = 0.5\text{ }\mu\text{m}$) device and a short channel ($L = 0.1\text{ }\mu\text{m}$) device ($t_{si} = 100\text{ nm}$, $t_{ox} = 10\text{ nm}$, $N_A = 1 \times 10^{16}\text{ cm}^{-3}$, $V_{GS} = -1\text{ V}$).

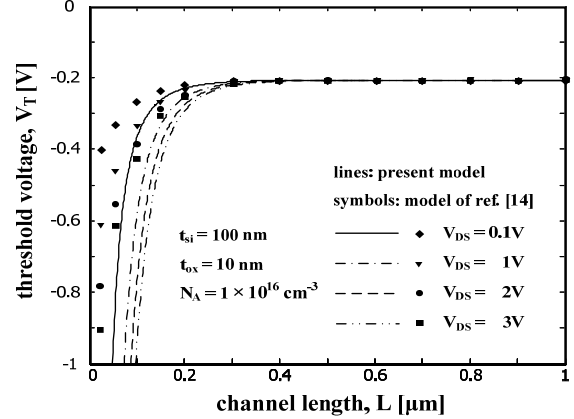


Fig. 4. Threshold voltage versus channel length for various values of drain voltage ($t_{si} = 100\text{ nm}$, $t_{ox} = 10\text{ nm}$, $N_A = 1 \times 10^{16}\text{ cm}^{-3}$).

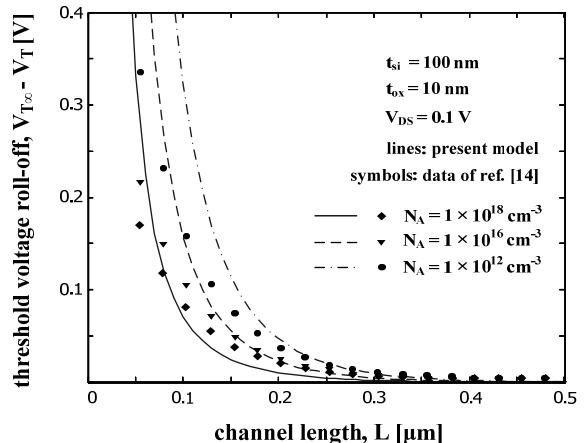


Fig. 5. Threshold voltage roll-off versus channel length for various values of doping density in the silicon core ($t_{si} = 100\text{ nm}$, $t_{ox} = 10\text{ nm}$, $V_{DS} = 0.1\text{ V}$).

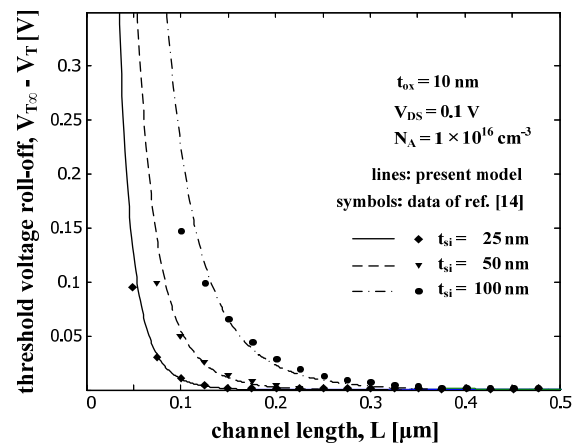


Fig. 6. Threshold voltage roll-off versus channel length for various values of silicon core diameter ($t_{ox} = 10\text{ nm}$, $N_A = 1 \times 10^{16}\text{ cm}^{-3}$, $V_{DS} = 0.1\text{ V}$).

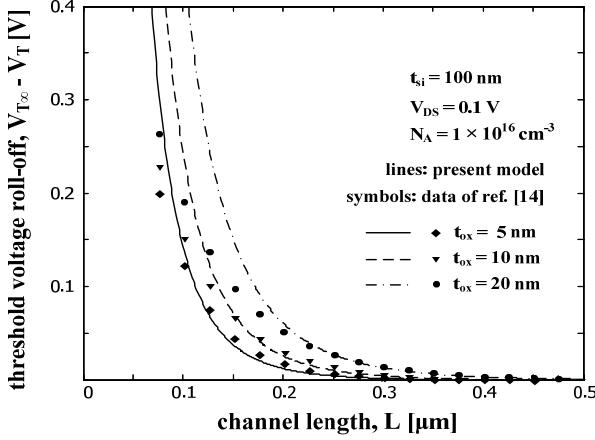


Fig. 7. Threshold voltage roll-off versus channel length for various values of oxide layer thickness ($t_{si} = 100 \text{ nm}$, $N_A = 1 \times 10^{16} \text{ cm}^{-3}$, $V_{DS} = 0.1 \text{ V}$).

IV. CONCLUSIONS

As shown in the above sample computation and discussion, the presented model can estimate fairly accurately the threshold voltage of a short channel fully depleted cylindrical/surrounding gate MOSFET. Updating iteratively the GCA-used potential expressions by taking into account the lateral variation of the surface potential, using the Bessel functions, and deriving the natural length expression, we can write the potentials in both oxide layer and silicon core fully two-dimensionally. Since the 2-D Laplace equation $(1/r)\partial(r\partial\psi/\partial r)/\partial r = -\partial^2\psi/\partial y^2$ may not be replaced with $(1/r)\partial(r\partial\psi/\partial r)/\partial r \approx 0$ in a fairly short and thick oxide layer, the presented fully two-dimensional potential will be more appropriate than the quasi-two-dimensional potential which has been used in the several analytical models. Without any approximation, the expression for the minimum surface potential can be obtained to derive the threshold voltage based upon the DIBL. Then the threshold voltage can be derived as a closed-form expression in terms of device parameters and applied voltages. From Eq. (40), the natural length can be derived exactly. However, by using Eq. (48), it can be derived more conveniently within a range of satisfactory accuracy. Compared with previously suggested several analytical models in which the equi-potential boundary conditions at both source-core and drain-core junction planes bring about rather complicated expressions, the presented model requires fewer approximations in the analytical procedure and can

derive the minimum surface potential and the threshold voltage accurately in a simpler manner. Therefore, the presented model may be used for estimating the threshold voltage of a short channel fully depleted cylindrical/surrounding gate MOSFET.

APPENDIX I

Using Eqs. (14, 15) step by step, we can obtain

$$f_1(r) = \frac{r_s^2}{2^2} (\rho^2 - 1), \quad (I-1)$$

$$f_2(r) = \frac{r_s^4}{2^4 \cdot (2!)^2} [\rho^4 - 1 - 4(\rho^2 - 1)], \quad (I-2)$$

$$f_3(r) = \frac{r_s^6}{2^6 \cdot (3!)^2} [\rho^6 - 1 - 9(\rho^4 - 1) + 27(\rho^2 - 1)], \quad (I-3)$$

$$g_1(r) = \frac{r_s^2}{2^2 \sigma} [(\rho^2 - 1)(1 + \sigma - \ln \rho) - K_1 \ln \rho], \quad (I-4)$$

$$g_2(r) = \frac{r_s^4}{2^6 \sigma} \left[\begin{aligned} & (\rho^4 - 1) \left(\frac{3}{2} + \sigma - \ln \rho \right) \\ & - 4(\rho^2 - 1) (2 + \sigma - \ln \rho - K_1 + K_1 \ln \rho) - K_2 \ln \rho \end{aligned} \right], \quad (I-5)$$

$$g_3(r) = \frac{r_s^6}{2^8 \sigma} \left[\begin{aligned} & \frac{1}{9} (\rho^6 - 1) \left(\frac{11}{6} + \sigma - \ln \rho \right) \\ & - (\rho^4 - 1) \left(\frac{5}{2} + \sigma - \ln \rho - \frac{3K_1}{2} + K_1 \ln \rho \right) \\ & + (\rho^2 - 1) \left(\frac{19}{2} + 3\sigma - 3\ln \rho - 8K_1 + K_2 + 4K_1 \ln \rho - K_2 \ln \rho \right) \\ & - K_3 \ln \rho \end{aligned} \right], \quad (I-6)$$

where $\rho = r/r_s$ and K_1 , K_2 , and K_3 are defined by

$$K_1 = \frac{1}{\sigma} (e^{2\sigma} - 1), \quad (I-7)$$

$$K_2 = \frac{3}{2\sigma} (e^{4\sigma} - 1) - 4K_1 (2 - K_1 + K_1 \sigma), \quad (I-8)$$

$$\begin{aligned} K_3 = & \frac{11}{54\sigma} (e^{6\sigma} - 1) - \frac{1}{\sigma} (e^{4\sigma} - 1) \left(\frac{5}{2} - \frac{3K_1}{2} + K_1 \sigma \right) \\ & + K_1 \left(\frac{19}{2} - 8K_1 + K_2 + 4K_1 \sigma - K_2 \sigma \right). \end{aligned} \quad (I-9)$$

Thus, considering Eqs. (21, 22, 25), we can have

$$a_1 = \frac{r_s^2}{2^2} \left(\frac{2\sigma}{\eta} - 2\sigma - 2 + K_1 \right), \quad (I-10)$$

$$a_2 = \frac{r_s^4}{2^4} \left(\frac{\sigma}{\eta} - \sigma - \frac{5}{2} + 2K_1 - \frac{K_2}{4} \right), \quad (\text{I-11})$$

$$a_3 = \frac{r_s^6}{2^6} \left(\frac{2\sigma}{3\eta} - \frac{2\sigma}{3} - \frac{23}{9} + \frac{5K_1}{2} - \frac{K_2}{2} + \frac{K_3}{4} \right). \quad (\text{I-12})$$

Using $e^x = 1 + x + x^2/2 + \dots$ into Eqs. (I-7, I-8, I-9), we get $K_1 = 2 + 2\sigma + 4\sigma^2/3 + \dots$, $K_2 = 6 + 12\sigma + 32\sigma^2/3 + \dots$, and $K_3 = 20/9 + 20\sigma/3 + 8\sigma^2 + \dots$. Hence, we can obtain

$$a_1 = \frac{r_s^2}{2^2} \left(\frac{2\sigma}{\eta} + \frac{4\sigma^2}{3} + \dots \right) > 0, \quad (\text{I-13})$$

$$a_2 = \frac{r_s^4}{2^4} \left(\frac{\sigma}{\eta} + \dots \right) > 0, \quad (\text{I-14})$$

$$a_3 = \frac{r_s^6}{2^6} \left(\frac{2\sigma}{3\eta} + \dots \right) > 0, \quad (\text{I-15})$$

$$a_2^2 - 3a_1a_3 = -\frac{r_s^8}{2^8} \left(\frac{3\sigma^2}{\eta^2} + \frac{8\sigma^3}{3\eta} + \dots \right) < 0. \quad (\text{I-16})$$

Then the discriminant D for the cubic equation of Eq. (28) can be obtained as

$$\begin{aligned} D = Q^3 + R^2 &= -\frac{1}{9^3} (a_1^2 + 3a_2)^3 + \frac{1}{54^2} (9a_1a_2 + 27a_3 + 2a_1^3)^2 \\ &= \frac{1}{108} (-4a_2^3 + 4a_1^3a_3 - a_1^2a_2^2 + 27a_3^2 + 18a_1a_2a_3) \\ &= \frac{1}{108} [(4a_2 + a_1^2)(3a_1a_3 - a_2^2) + a_1^3a_3 + 27a_3^2 + 6a_1a_2a_3] > 0. \end{aligned} \quad (\text{I-17})$$

Thus, λ given by Eq. (29) is the unique positive solution of Eq. (28).

APPENDIX II

Replacing k with $k-1$ in Eqs. (43, 44), we have

$$J_0^{(k-1)}(x) = \mu_{k-1}(x)J_0(x) + \nu_{k-1}(x)J_1(x), \quad (\text{II-1})$$

$$Y_0^{(k-1)}(x) = \mu_{k-1}(x)Y_0(x) + \nu_{k-1}(x)Y_1(x). \quad (\text{II-2})$$

Differentiating Eqs. (II-1, II-2) with respect to x yields

$$\begin{aligned} \frac{dJ_0^{(k-1)}}{dx} &= J_0^{(k)}(x) = \frac{d\mu_{k-1}}{dx} J_0(x) - \mu_{k-1}(x)J_1(x) \\ &+ \frac{d\nu_{k-1}}{dx} J_1(x) + \nu_{k-1}(x) \left[J_0(x) - \frac{J_1(x)}{x} \right], \end{aligned} \quad (\text{II-3})$$

$$\begin{aligned} \frac{dY_0^{(k-1)}}{dx} &= Y_0^{(k)}(x) = \frac{d\mu_{k-1}}{dx} Y_0(x) - \mu_{k-1}(x)Y_1(x) \\ &+ \frac{d\nu_{k-1}}{dx} Y_1(x) + \nu_{k-1}(x) \left[Y_0(x) - \frac{Y_1(x)}{x} \right]. \end{aligned} \quad (\text{II-4})$$

Then equating Eqs. (43, II-3), we can get Eqs. (45, 46). Also we can get Eqs. (45, 46) by equating Eqs. (44, II-4).

REFERENCES

- [1] Takato H., Sunouchi K., Okabe N., Nitayama A., Hieda K., Horiguchi F., Masuoka F., "High performance CMOS surrounding gate transistor (SGT) for ultra high density LSI's," *IEDM Tech. Dig.*, pp.222-225, 1998.
- [2] Sunouchi K., Takato H., Okabe N., Yamada T., Ozaki T., Inoue S., Hashimoto K., Hieda K., Nitayama A., Horiguchi F., Masuoka F., "A surrounding gate transistor (SGT) cell 64/256 Mbit DRAMs," *IEDM Tech. Dig.*, p.23, 1989.
- [3] Takato H., Sunouchi K., Okabe N., Nitayama A., Hieda K., Horiguchi F., Masuoka F., "Impact of surrounding gate transistor (SGT) for ultra high density LSIs," *IEEE Trans. Electron Devices*, Vol.38, pp.573-578, 1991.
- [4] Nitayama H., Takato H., Okabe N., Sunouchi K., Hieda K., Horiguchi F., Masuoka F., "Multi-pillar surrounding gate transistor (M-SGT) for compact and high speed circuits," *IEEE Trans. Electron Devices*, Vol.38, pp.579-583, 1991.
- [5] Miyano S., Hirose M., Masuoka F., "Numerical analysis of a cylindrical thin-pillar transistor (CYNTHIA)", *IEEE Trans. Electron Devices*, Vol.39, pp.1876-1881, 1992.
- [6] Watanabe S., Tsuchida K., Takashima D., Oowaki T., Nitayama A., Hieda K., Takato H., Sunouchi K., Horiguchi F., Ohuchi K., Masuoka F., Hara H., "A novel circuit technology with surround gate transistors (SGT) for ultra-high density DRAM's", *IEEE J. Solid State Circuits*, Vol.30, pp.960-971, 1995.
- [7] Endoh T., Nakamura T., Masuoka F., "An accurate

- model of fully-depleted surrounding gate transistor (FD-SGT)", *IEICE Trans. Electron.*, Vol.E80-C, pp.905-910, 1997.
- [8] Endoh T., Nakamura T., Masuoka F., "An analytical steady-state current-voltage characteristics of a short channel fully depleted surrounding gate transistor (FD-SGT)", *IEICE Trans. Electron.*, Vol.E80, pp.911-917, 1997.
- [9] Auth C.P., Plummer J.D., "Scaling theory for cylindrical, fully-depleted, surrounding gate MOSFET's", *IEEE Electron Device Lett.*, Vol.18, No.2, pp.74-76, 1997.
- [10] Jang S.L., Liu S.S., "An analytical surrounding gate MOSFET model", *Solid State Electronics*, Vol.42, No.5, pp.721-726, 1998.
- [11] Oh S.H., Monroe D., Hergenrother J.M., "Analytic description of short-channel effects in fully-depleted double-gate and cylindrical, surrounding-gate MOSFETs", *IEEE Electron Device Lett.*, Vol.21, No.9, pp.445-447, 2000.
- [12] Kranti A., Haldar S., Gupta R.S., "An accurate 2D analytical model for short channel thin film fully depleted cylindrical/surrounding gate (CGT/SGT) MOSFET", *Microelectronics Journal*, Vol.32, pp.305-313, 2001.
- [13] Kranti A., Haldar S., Gupta R.S., "Analytical model for threshold voltage and I-V characteristics of fully depleted short channel cylindrical/surrounding gate MOSFET", *Microelectronic Engineering*, Vol.56, pp.241-259, 2001.
- [14] Chiang T.K., "A new two-dimensional threshold voltage model for cylindrical, fully-depleted, surrounding gate (SG) MOSFETs", *Microelectronics Reliability*, Vol.47, pp.379-383, 2007.
- [15] Murray R. Spiegel, John Liu, *Mathematical Handbook of Formulas and Tables*, p.33, 1968, 2nd ed., McGraw-Hill
- [16] Suh C.H., "A simple analytical model for the front and back gate threshold voltages of a fully-depleted asymmetric SOI MOSFET", *Solid State Electronics*, Vol.52, pp.1249-1255, 2008.
- [17] Suh C.H., "Analytical model for deriving the threshold voltages of a short gate SOI MESFET with vertically non-uniformly doped silicon film", *IET Circuits, Devices, and Systems*, Vol.4, No.6, pp.525-530, 2010.



Chung Ha Suh was born in Daegu, Korea, in 1946. He received the B. S. degree from Seoul National University in 1969, Department of Electronic Engineering, the M. S. degree from Hongik University in 1975, and the Ph. D. degree in the area of semiconductor device physics from Seoul National University in 1981. In 1976 he joined the Department of Electronic Engineering, Hongik University, and served there as an Assistant Professor until 1978, and was promoted to a Full Professor in February, 1987. He was at the University of Minnesota from 1979 to 1980 as a visiting scholar and joined the Post Doc. program at the University of Pennsylvania from 1983 to 1984. At Hongik University, he served as Dean of Research Affairs and Dean of Graduate School of Industrial Information Technology from 1991 to 1999. His areas of interest are solid-state electronics and integrated circuit. He has published two text books in the area of physical electronics, and several papers in the IEEE TRANSACTIONS ON ELECTRON DEVICES, the *Journal of Applied Physics*, Solid-State Electronics, and other technical publications.

Dr. Suh is a life-long member of the Korean Institute of Electronics Engineers and a member of IEEE.